Postprint of: Chromá R., Vilková M., Shepa I., Makoś-Chełstowska P., Andruch V., Investigation of tetrabutylammonium bromide-glycerol-based deep eutectic solvents and their mixtures with water by spectroscopic techniques, JOURNAL OF MOLECULAR LIQUIDS (2021), 115617, DOI: 10.1016/j.molliq.2021.115617

Investigation of tetrabutylammonium bromide-glycerol-based deep eutectic solvents and their mixtures with water by spectroscopic techniques

Renáta Chromá [a], Mária Vilková [b], Ivan Shepa [c], Patrycja Makoś-Chełstowska [d], Vasil Andruch [a]

[a] *Department of Analytical Chemistry, Institute of Chemistry, Faculty of Science, Pavol Jozef Šafárik University in Košice, SK-04154 Košice, Slovakia*

[b] *Laboratory of NMR, Institute of Chemistry, Faculty of Science, Pavol Jozef Šafárik University in Košice, SK-04154, Košice, Slovakia*

[c] *Institute of Materials Research, Slovak Academy of Sciences, SK-04001 Košice, Slovakia*

[d] *Department of Process Engineering and Chemical Technology, Gdansk University of Technology, Gdansk, PL-80-233 Gdańsk, Poland*

Abstract

Deep eutectic solvents (DES) are formed by an acceptor and a donor of hydrogen bonds. They are generally considered as a possible alternative to hazardous organic solvents in various fields. Very recently they have also appeared in analytical chemistry, used mainly for the separation of analytes before instrumental quantification. For the development of new extraction procedures, it is important, among other things, to understand the mechanism of the extraction process itself. In this study we present NMR, IR and Raman spectroscopy studies of TBAB-Gly-based DESs at various HBA:HBD molar ratios for the neat DES as well as the DES mixed with various amounts of added water to better understand the mechanism of DES formation, intermolecular interactions in DES and the interaction of the DES with water, which have not yet been studied in detail. The obtained results indicate that hydrogen bonds between TBAB and Gly exist in the DESs at all molar ratios (1:2; 1:3; 1:4). A small amount of water added to the DES structure provides the establishment of an H-bond network, which does not weaken the existing H-bonds between the HBA and HBD, thus creating a stable supramolecular structure. However, further increasing of water amount provide to weakened of hydrogen bonds between TBAB and Gly.

Keywords: Deep eutectic solvents; Tetrabutylammonium bromide; Glycerol; NMR spectroscopy, IR spectroscopy, Raman spectroscopy

Abbreviations

DES, Deep eutectic solvent;
DLLME, Dispersive liquid-liquid microextraction;
FT-IR, Fourier transform infrared spectroscopy;
HBA, Hydrogen bond acceptor;
HBD, Hydrogen bond donor;
HPLC-FLD, High-performance liquid chromatography with fluorescence detection;
HS-SDME, Headspace single-drop microextraction;
IL, Ionic liquid;
LPME, Liquid-phase microextraction;
MS-FAAS, Micro-sampling flame atomic absorption spectrometry;
NMR, Nuclear magnetic resonance;
NOESY, Nuclear Overhauser effect spectroscopy;
PAH, Polycyclic aromatic hydrocarbons;

ROESY, Rotating-frame nuclear Overhauser effect spectroscopy;
SFO, Solidification of floating organic droplet;
TBAB, Tetrabutylammonium bromide;
TBAC, Tetrabutylammonium chloride;
UA-, Ultrasound-assisted;
USAEME, Ultrasound-assisted emulsification microextraction;
VA-, Vortex-assisted.

1 Introduction

Since the 1970s, the term "sustainable development", which presupposes development in such a way that improvements in human well-being are also linked to the preservation of nature, has been a subject of discussion. Therefore, great emphasis is currently placed on the continuous reduction of environmental burdens and the gradual introduction of environmentally friendly production technologies based on the rule "It is better to prevent the generation of waste than to dispose of it" [1]. One possible way to achieve this goal is to replace conventional hazardous solvents with less dangerous, biodegradable, more eco-friendly ones which at the same time are more efficient. In this context, new types of solvents, such as ionic liquids (IL) [2], switchable hydrophilicity solvents (SHS) [3, 4] and deep eutectic solvents (DES) [5], should be mentioned. Although the use of DES in analytical chemistry is still in its infancy, the number of both research and review papers focusing on their use has been increasing in recent years [6].

One frequently used HBA is tetrabutylammonium bromide (TBAB). For analytical chemistry purposes, DESs based on TBAB as the HBA with a variety of HBDs, such as long-chain alcohols (butanol [7, 8], amyl alcohol [9], heptanol [9], octanol [7-9], decanol [7, 9], dodecanol [7-9], oleyl alcohol [8]); polyhydric alcohols (ethylene glycol [10, 11], glycerol [11]); cyclohexanol [8]; carboxylic acids (formic acid [10-12], acetic acid [10, 11, 13], propionic acid [10, 13], butyric acid [13], hexanoic acid [7, 8], octanoic acid [8, 13], decanoic acid [8, 13-16], lactic acid 1:2 [7], acrylic acid [13]); and fatty acids (oleic acid [13]), have been studied. Besides TBAB, DESs composed of TBAC as the HBA and various HBDs, such as dodecanol [7], hexanoic acid [7] and decanoic acid [14, 16, 17], have also been studied.

Selected examples of microextraction procedures using TBAB-based DESs in analytical chemistry are shortly discussed below and are shown in Table 1. A series of hydrophobic DESs consisting of TBAB and carboxylic acids (*oleic acid, decanoic acid, octanoic acid, propionic acid, acrylic acid, acetic acid and butyric acid*) in a 1:2 molar ratio were prepared and investigated as an extraction solvent for PAHs from water samples [13]. Analysis of the chemical structures of the synthesized DESs was carried out by FT-IR analysis. Among the studied DESs, the highest recoveries for PAHs were obtained using TBAB-decanoic acid [13]. Soylak's group investigated TBAC/TBAB-decanoic acid DESs for USAEME separation and preconcentration of quercetin in vegetable and fruit samples [14]; Brown HT (E155) in cake, artificial urine and water samples [15]; and tartrazine in water, drug and beverage samples [16], followed by UV-Vis determination; as well as nickel in water, food and cigarette samples prior to MS-FAAS determination [17]. DESs made up of TBAB and long-chain alcohols were investigated for HS-SDME of terpenes from six spices (*cinnamon, cumin, fennel, clove, thyme and nutmeg*). The DES composed of TBAB and dodecanol at a molar ratio of 1:2 showed the highest extraction efficiency [7].

The decomposition of DESs was applied in DLLME procedures for dispersion of the extraction solvent instead of a conventional dispersive solvent. Shishov et al. reported a DLLME procedure for the extraction of bisphenol-A from beverage samples, followed by HPLC-FLD. In this approach, the dispersion of the extraction solvent (octanol) in an aqueous sample and at the same time the extraction

of the analyte takes place as a result of the decomposition of a DES consisting of TBAB-formic acid 1:2 during injection of the aqueous sample into a homogeneous octanol-DES mixture [11]. Later, this approach was applied for the development of an automated in-syringe DLLME procedure for UV–Vis determination of chromium(VI) in beverage samples using an extraction solvent (1-octanol) and a dispersive solvent (TBAB-formic acid, 1:4 molar ratio) containing 1,5-diphenylcarbazide as the complex-forming reagent [12]. Similarly, El-Deen et al. reported a DLLME-SFO method for preconcentration of steroids in water samples using TBAB-acetic acid 1:2 DES as the dispersive solvent [10]. Decomposition of a DES (TBAB-heptanol 1:2) was also applied for the determination of 17β-estradiol in transdermal gel samples [9].

Table 1. Examples of the application of TBAB-based DESs in analytical chemistry.

Analyte	Matrix	DES and molar ratio	Procedure	Detection	LR/LOD	Ref.
PAHs	Water	TBAB-decanoic acid 1:2	UA-DLLME-SFO	HPLC-FLD	LR: up to 5000 ng L^{-1} LOD: 0.7-6.6 ng L^{-1}	[13]
Quercetin	Fruits and vegetables	TBAC-decanoic acid 1:3	USAEME	UV-VIS, 370 nm	LR: 67-838 μg L^{-1} LOD: 18.8 μg L^{-1}	[14]
Brown HT	Cake, artificial urine and water	TBAB-decanoic acid 1:2	UA-LPME	UV-VIS, 470 nm	LR: – LOD: 0.23 μg mL^{-1}	[15]
Tartrazine	Water, drug and beverage	TBAB-decanoic acid 1:3	UA-LPME	UV-VIS, 430 nm	LR: 0.25-2.60 mg L^{-1} LOD: 0.084 mg L^{-1}	[16]
Ni(II)	Water, food and cigarette	TBAC-decanoic acid 1:3	UA-LPME	MS-FAAS	LR: – LOD: 0.13 μg L^{-1}	[17]
Antibiotics	Water	Tricaprylylmethylammonium-octanol 1:4	VA-LPME	HPLC-UV	LR: 0.1-50 μg mL^{-1} LOD: 0.016 and 0.024 μg mL^{-1}	[8]
Steroids	Water	TBAB-acetic acid 1:2	DLLME-SFO	HPLC-UV	LR: 0.01-20.0 μg mL^{-1} LOD: 1.0-9.7 ng mL^{-1}	[10]
Bisphenol-A	Beverage	TBAB-formic acid 1:2	DLLME	HPLC-FLD	LR: 0.001-1 mg L^{-1} LOD: 0.0003 mg L^{-1}	[11]
Cr(VI)	Beverage	TBAB-formic 1:4	In-syringe DLLME	UV-Vis	LR: – LOD: 0.2 μg L^{-1}	[12]
17β-estradiol	Transdermal gels	TBAB-heptanol 1:2	DLLME	HPLC-UV	LR: 0.5-100 mg L^{-1} LOD: 0.15 mg L^{-1}	[9]
Terpenes	Plant	TBAB-dodecanol 1:2	HS-SDME	GC-MS	LR: 1-500 μg g^{-1} LOQ: 0.47 to 86.40 μg g^{-1}	[7]

LR – Linear range; LOD – Limit of detection.

It is clear that TBAB-based DESs have been used for analyses of several kinds of samples, such as water, beverage, fruit, vegetable, food and drugs, using various LPME techniques followed by HPLC-UV/FLD detection, UV-Vis spectrophotometric, GC-MS and FAAS quantification. Of course, analysts are particularly interested in the analytical parameters of the methods and usually spend less time and effort studying the mechanism of the process [18]. This kind of information, however, can be very helpful in the development of new analytical procedures.

Therefore, in this study we present NMR, IR and Raman spectroscopy studies of TBAB-Gly-based DESs at various HBA:HBD molar ratios for the neat DES as well as the DES mixed with various amounts of added water to better understand the mechanism of DES formation, intermolecular interactions in DES and the interaction of the DES with water, which have not yet been studied in detail. DES composed of tetrabutylammonium bromide and glycerol was selected because these components are easily available and inexpensive, as well as due to the proven application potential of DESs in analytical chemistry.

2 Experimental

2.1 Materials and chemicals

Tetrabutylammonium bromide (TBAB; Lachema, Brno, Czech Republic) and glycerol (Gly; Sigma-Aldrich, Malaysia, ≥ 99, 5%) were used as supplied. The chemical structures and numbering of atoms used in the NMR experiments are presented in Fig. 1.

2.2 Apparatus

NMR measurements were performed on a Varian VNMRS 600 spectrometer operating at a ^{1}H frequency of 599.86 MHz with a ^{1}H-^{19}F/^{15}N-^{31}P 5mm PFG OneNMR Probe. NMR tubes 5 mm in diameter and 7 inches long were used. For DMSO-d_6 diluted DES, DMSO-d_6 was used as a solvent and reference standard (^{1}H NMR: 2.50 ppm (quintet, J_{HD} = 1.9 Hz, DMSO-d_5); ^{13}C NMR: 39.52 ppm (septet, J_{CD} = 21.0 Hz, DMSO-d_6). For neat and water-diluted DES, benzene-d_6 (a 2-mm capillary tube placed at the center of the 5-mm sample tube) was used as a reference standard (^{1}H NMR: 7.16 ppm (quintet, J_{HD} = 1.2, 0.2 Hz, benzene-d_5); ^{13}C NMR: 128.0 ppm (triplet, J_{CD} = 24.3 Hz, benzene-d_6). ^{1}H and ^{1}H,^{1}H-NOESY were recorded at 298 K. The mixing time was adjusted for TBAB:Gly (1:4), and the 2D NOESY spectra were recorded with mixing times of 100, 200, 400, 600, 800 and 1000 ms. The 2D ROESY spectra were recorded with mixing time of 100, 300 and 500 ms. Peaks were identified and spectra were processed using the software MNova.

Fourier transform infrared spectroscopy (FT-IR) at a resolution of 4 cm^{-1} was performed with a Nicolet 6700 FT-IR spectrometer (Thermo Scientific) using an ATR Smart orbit device. Raman spectroscopy of the tested specimens was carried out using a Raman XploRA microscope by HORIBA Jobin Yvon (with an integrated high-intensity laser, IMR SAS, Slovakia). Raman spectra were recorded with an excitation laser wavelength of 532 nm in the range from 100 to 4000 cm^{-1}. Laser power was adjusted for each sample to obtain a high-intensity signal and avoid sample damage.

2.3 Preparation of DESs

The deep eutectic solvents were prepared by mixing the desired amounts of the two components at an elevated temperature. The required amounts of TBAB as the HBA and glycerol as the HBD in various molar ratios (1:2, 1:3 and 1:4) were introduced into laboratory glass vials. The mixture was stirred at 300 rpm and a temperature up to 90 °C with a temperature controlled magnetic stirrer (model RHD, IKA, Germany) until a homogenous liquid was formed. In the next step melting point (MP) of DESs were studied visually at atmospheric pressure by means of cooling TBAB:Gly in various molar ratio to -50 °C, followed by a temperature increase at 0.5 °C/min. The initial temperature at which the phase change of DES occurred was taken as the MP. The DES at 1:2 molar ratio tended to form a suspension after cooling to room temperature (Table 2); therefore, only DESs at 1:4 and 1:3 molar ratios were subjected to detailed investigations. Subsequently, 10, 20, 50, 80 and 90% (v/v) water was added to DESs.

Table 2. DESs studied in this work.

DES	Molar ratio	MP [°C]	Appearance
TBAB:Gly	1:2	-6	Slightly light-yellow viscous liquid with particles in suspension after cooling to room temperature
TBAB:Gly	1:3	-14	Slightly light-yellow viscous liquid with particles in suspension after 24 h standing at room temperature
TBAB:Gly	1:4	-40	Slightly light-yellow viscous liquid

2.4 Theoretical FT-IR and Raman vibrational bands

FT-IR and Raman vibrational bands calculations were made in the following steps: (1) The structures of DESs and DES-water complexes were generated by Avogadro 1.2.0 program [19]. (2) Molecular geometry optimization and vibrational frequencies of DESs, and DES-water complexes were performed based on the Beck3–Lee–Yang–Parr (B3LYP) level with the use of the 6-311+G** basis set, by means of Orca 4.2.1 software [20, 21]. (3) The atomic displacements for each vibrational mode of DESs and DES-water complexes were calculated, using Multiwfn 3.7 program [22]. (4) The calculated frequencies were scaled using two factors 0.958 and 0.983 based on previous studies [23].

3 Results and Discussion

3.1 NMR study of the structure of DESs

The ^{1}H NMR, ^{13}C NMR, NOESY and ROESY experiments were performed to determine the structure of the examined DESs as well as their stability with increasing temperature. To exclude the influence of deuterated solvent, the internal double-tube method was employed in the ^{1}H and ^{13}C NMR experiments to obtain accurate chemical shifts. A 2-mm capillary tube with benzene-d_6 was placed at the center of the 5-mm sample tube [24].

Fig. 1 shows the ^{1}H and ^{13}C NMR of neat TBAB:Gly (1:4) and TBAB:Gly (1:3). The ^{1}H NMR spectra are characterized by broad lines due to the inherent viscosity of the DESs. Nevertheless, all the ^{1}H NMR signals for the DES at both studied molar ratios are separated.

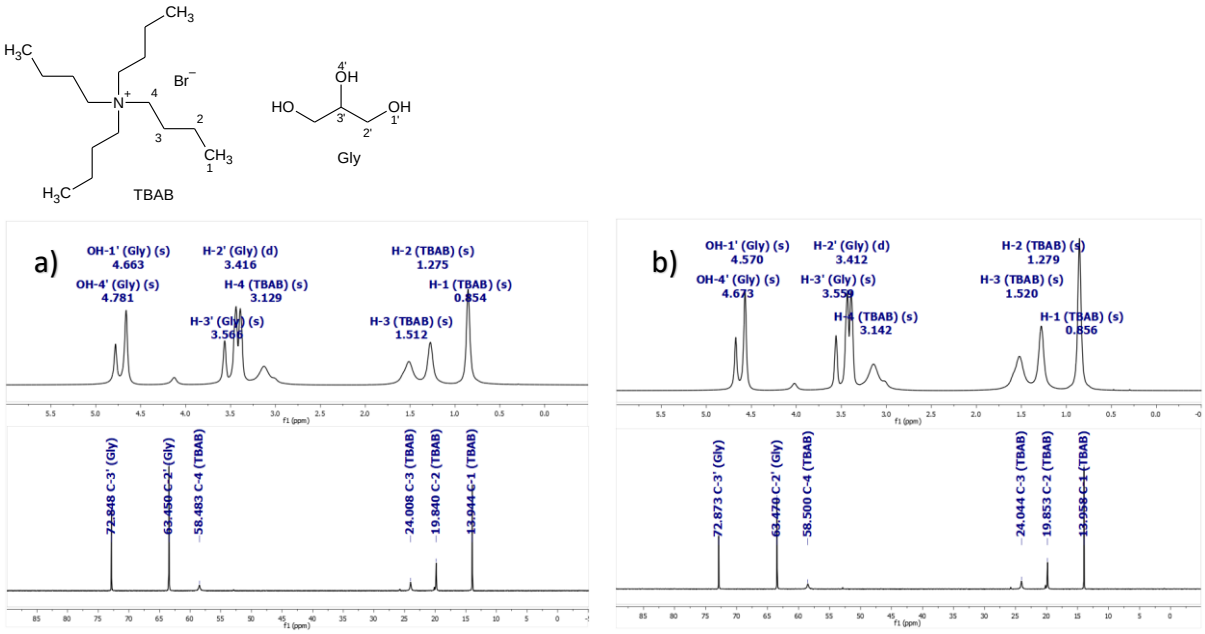

Fig. 1. ^{1}H (600 MHz) and ^{13}C NMR (150 MHz) spectra of a) TBAB:Gly (1:4), b) TBAB:Gly (1:3), and the chemical structures and numbering of atoms. Spectra were referenced to benzene-d_6 (capillary insert).

The ^{1}H NMR spectra (Fig. 2, Table S1) for both DESs were recorded at three temperatures (25, 40, 60 °C and after cooling) to evaluate the effect of temperature on viscosity and thermal stability. It is obvious that the chemical environment of the nuclei has changed. With increasing temperature, all the lines have been shifted upfield and became sharper and split. Therefore, we can conclude that the H-bonds have been weakened. Upon cooling, the H-bonds re-formed and the supramolecular structure was rebuilt.

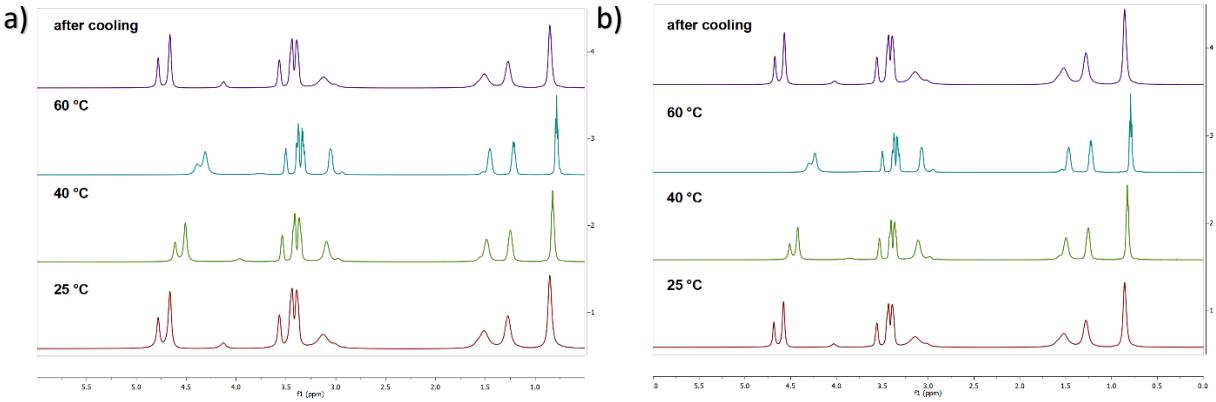

Fig 2. ^{1}H NMR (600 MHz) spectra of neat a) TBAB:Gly (1:4) and b) TBAB:Gly (1:3) measured at 25, 40, 60 °C and after cooling. Spectra were referenced to benzene-d_6 (capillary insert).

The NOESY and ROESY experiments were performed to investigate the interactions between the components of the DESs and thus to understand their supramolecular structure. NOE cross-peaks normally result from dipolar cross-relaxation of neighboring spins through space, and its signal intensities are a function of the distances between interacting nuclei. In viscous samples, such as a DES, the tumbling rate of the components is reduced, spin diffusion is highly efficient and dipolar interactions become considerable. The nuclear Overhauser effect (NOE) becomes large and of negative sign (positive cross-peaks). With a longer mixing time the cross-peaks become more intense, which evidences the existence of interactions between the protons from the different species throughout the space. The spin diffusion effect is discarded when using the ROESY experiment and shows only negative cross-peaks (positive NOE) [25, 26].

The extreme viscosity of the sample is sufficient to make the correlation time very long, such that the TBAB:Gly complex behaves like a very large macromolecule in which spin diffusion is efficient. In neat DESs, cross-peaks showing intermolecular NOESY interactions (negative NOE) and ROESY interactions (positive NOE) are observed as expected (Fig. 3).

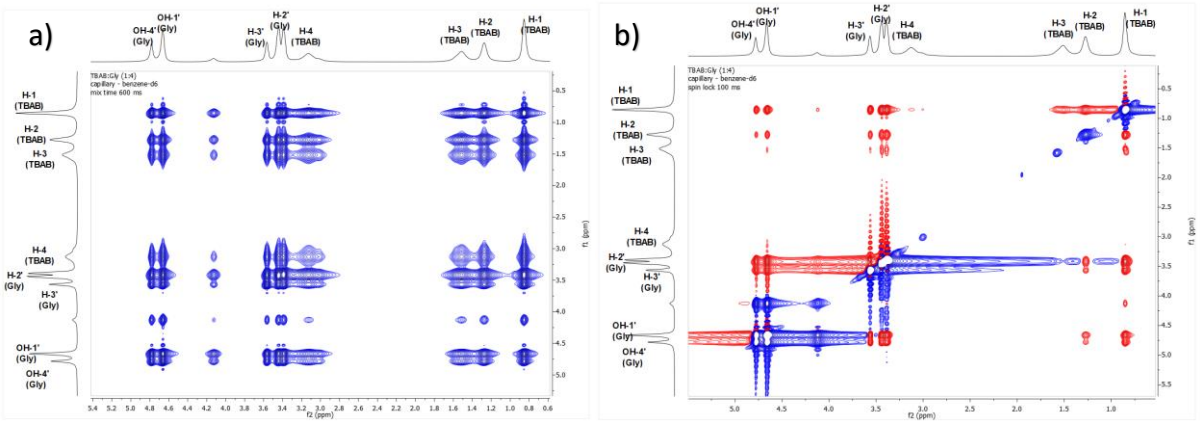

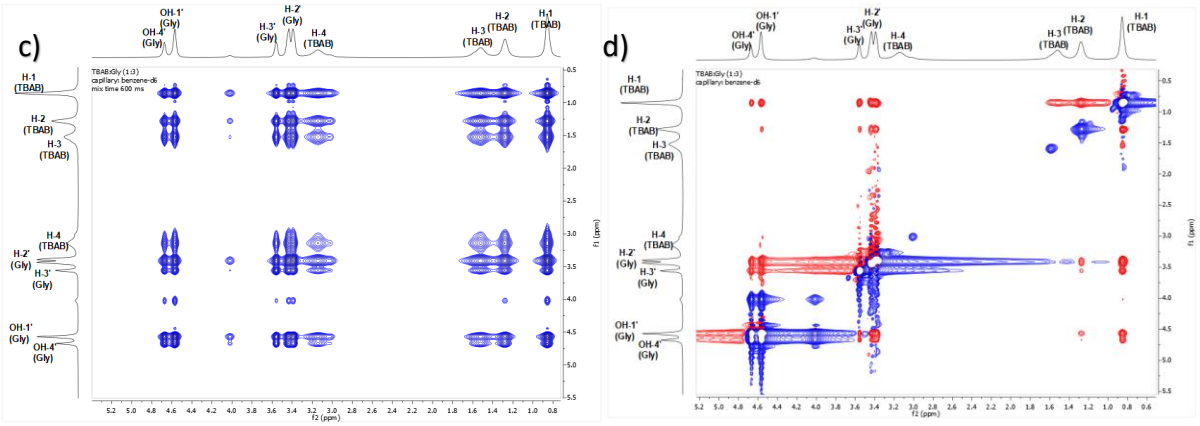

Fig. 3. NOESY (mix time 600 ms, capillary insert: benzene-d_6) (a, c) and ROESY (spin lock 100 ms, capillary insert: benzene-d_6) (b, d) spectra of TBAB:Gly (1:4) (a, b) and TBAB:Gly (1:3) (c, d).

3.2 NMR study of the effect of water on the structure of DESs

Water can have both a positive and negative effect on DESs [18]. On the one hand, water in moderate amounts contribute to establishing the H-bond network [26, 27]. On the other hand, an increase of the water content weakens the supramolecular structure until the point of rupture of the H-bonds and collapse into an aqueous solution. Therefore, the effect of water on the structure of DESs was investigated using NMR spectroscopy.

The ^{1}H NMR spectra of aqueous solutions of DESs containing 10, 20, 50, 80 and 90% (v/v) water exhibited a downfield shift of the TBAB and Gly signals (Fig. 4, Fig. S1, and Table S2). The upfield shift of the TBAB and Gly signals in neat DES indicates strong interactions between the TBAB Br atom and hydroxyl protons of Gly. The dilution shifts the Gly hydroxyl protons downfield. This can be explained by the formation of H-bonds between the Gly hydroxyl protons and water. This is indicative of the rupture of hydrogen bonds of the DES during dilution, with increased hydration of the TBAB and Gly.

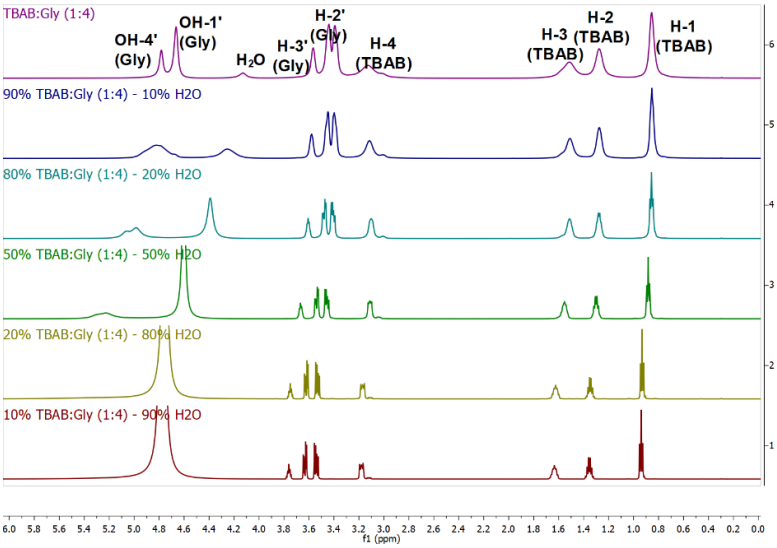

Fig. 4. ^{1}H NMR (600 MHz, capillary insert: benzene-d_6) spectra of TBAB:Gly (1:4) and TBAB:Gly (1:4)–H_2O mixtures.

The spin-spin relaxation time constant T_2 values could be further evidence of the disintegration of the supramolecular structure. T_2 is a dynamic NMR parameter and depends on molecular motion processes. Small, rapidly rotating molecules have longer T_2 times and sharper NMR lines, while larger

molecules rotate slowly and have shorter T_2 times and broader NMR lines [28]. Although we do not have a relaxation time constant for T_2 values, from the full width at half maximum (fwhm) (Fig. 5) of the ^{13}C NMR signals (Figs. S2 and S3, Table S3) we can conclude that with an increasing proportion of water in the DES sample, the ^{13}C NMR lines become sharper (Fig. 5) due to the decrease in the viscosity of the sample and marked rotational dynamics of the free components. The line widths of the C–3 and C–4 carbon signals of the TBAB are the most affected.

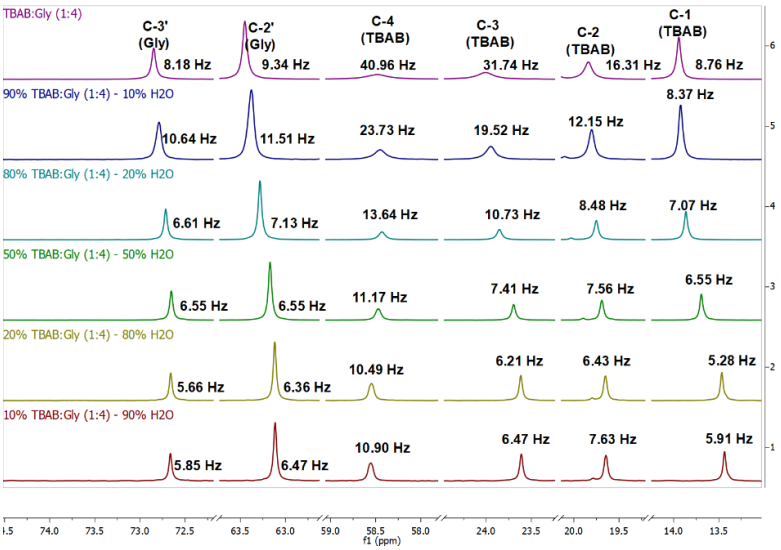

Fig. 5. ^{13}C NMR (150 MHz, capillary insert: benzene-d_6) spectra of TBAB:Gly (1:4)–H_2O mixtures. For each peak the fwhm is reported. Spectra were recorded with 64 scans and processed using an exponential filter (LB = 5 Hz).

The change in the supramolecular structure of DESs due to the addition of water was monitored by NOESY and ROESY experiments. In the NOESY experiment of 80% TBAB:Gly (1:3)–20% H_2O (Fig. 6a) and 80% TBAB:Gly (1:4)–20% H_2O (Fig. S4a), the negative NOE between the TBAB and Gly is still observable. In addition, positive NOE between the OH and H-2' and H-3' protons of Gly and water protons and the H-2' and H-3' protons of Gly appear. We suppose that the DES maintains its properties and water is a part of supramolecular structure of the DES. This fact is also supported by ROESY spectra (Fig. 6b, Fig. S4b). With an increased proportion of water (50% TBAB:Gly (1:3)–50% H_2O), negative NOE disappeared and positive signals between H_2O and Gly and H_2O and TBAB are observed (Fig. 6c). In the ROESY spectrum only intramolecular cross peaks between TBAB protons and intermolecular cross peaks between water and TBAB appear (Fig. 6d).

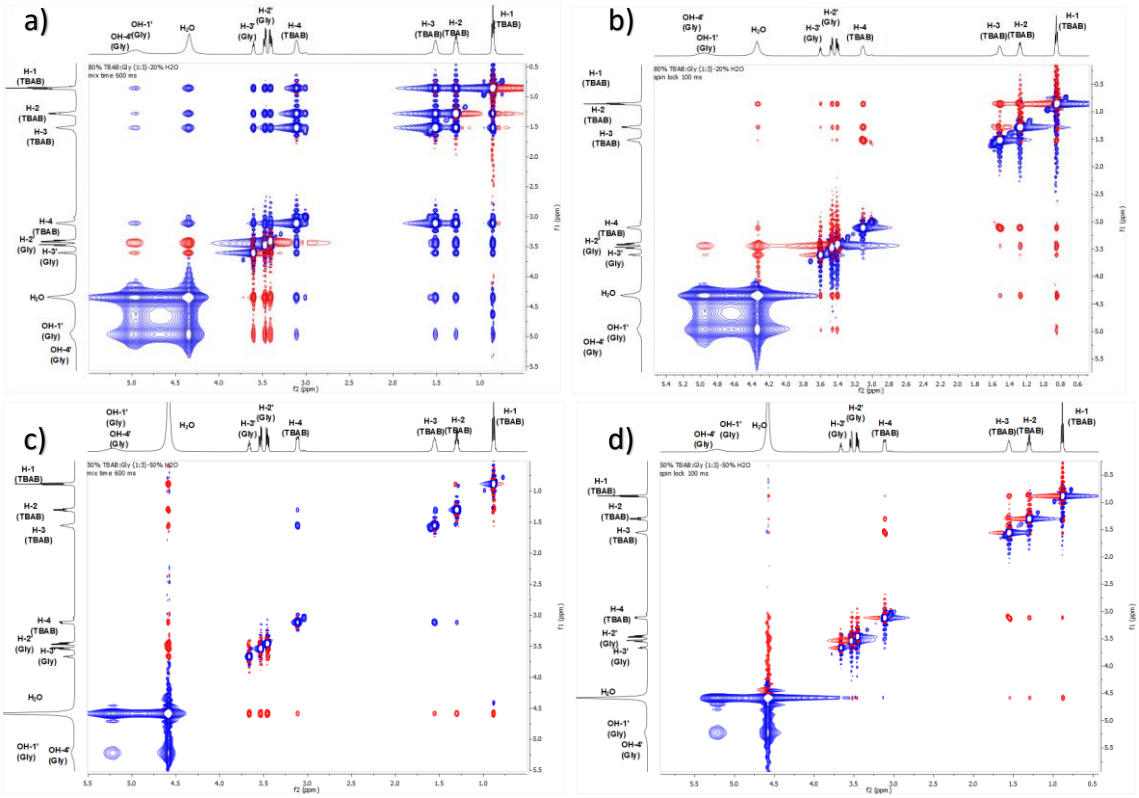

Fig. 6. NOESY (mix time 600 ms, capillary insert: benzene-d_6) (a, c) and ROESY (spin lock 100 ms, capillary insert: benzene-d_6) (b, d) spectra of 80% TBAB:Gly (1:3)–20% H_2O (a, b), and 50% TBAB:Gly (1:3)–50% H_2O (c, d).

The results (^1H, ^{13}C NMR and NOESY spectra) demonstrated that intensive H-bonds between TBAB and Gly are weakened by dilution with water. However, the supramolecular structure remains preserved to some extent even at 50% water content (Figs. 5 and 6).

3.3 Effect of water in DMSO-d_6

Studying the results of other authors, we found that DMSO-d_6 has been used many times as a solvent for confirming the structure of a DES by NMR. Usually, a small amount of DES was dissolved in DMSO-d_6. The peaks of the individual DES components were relatively sharp and the splitting of multiplets appeared. Nevertheless, the authors did not anticipate the decomposition of the DES by a deuterated solvent DMSO-d_6. Water is a common “impurity” of deuterated solvents and some amount of water are always present. Although only a small amount of water is present, this can still significantly affect the solute. DMSO-d_6 is highly hygroscopic, so we tried to analyze the effect of wet DMSO-d_6 on the structure and behavior of the studied DESs. A change in the chemical shifts of the DES constituent protons with increased DMSO-d_6 content in the DESs (Table S4) reflects a change in the environment of the DESs components. The upfield shift of H_2O (from DMSO-d_6) and the hydroxyl proton signals is observed as dilution increases from 10 up to 80% DMSO-d_6.

The chemical shift of the water protons dependent on the water concentration can offer us direct information about the H-bonding strength of water: the larger chemical shift, the stronger H-bond [24]. It can be seen from the ^1H NMR spectra (Fig. 7 and Fig. S5) that the chemical shift of the water protons is higher at the lower concentration of water in the samples, which means that just at this condition the water forms stronger H-bonds with the DES. This suggests that water is part of the supramolecular structure of the DES. By comparing the chemical shifts of the water protons (Table S4)

of the individual DESs, the stronger H-bonds are formed in TBAB:Gly (1:4). Another fact is worth mentioning: the negative charge of the Br atom as the electron-donator of the H-bond increases the electron density around the hydrogen atom of water, which is responsible for the upfield shift of the water protons in pure TBAB (dissolved in DMSO-d_6) in comparison with pure Gly (dissolved in DMSO-d_6) or DES (Fig. 7 and Fig. S5).

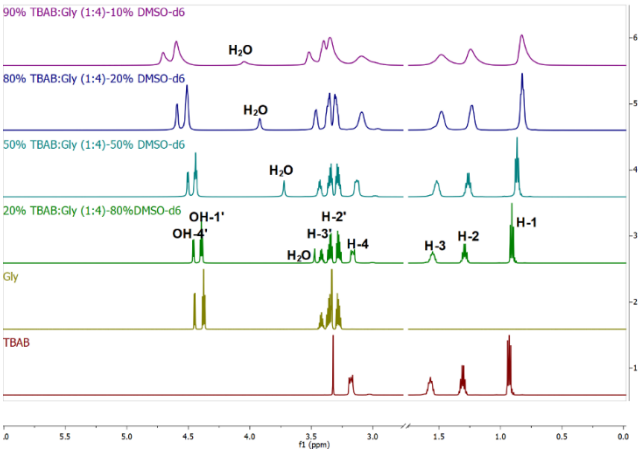

Fig. 7. ^{1}H NMR (600 MHz) spectra of individual components TBAB, Gly and TBAB:Gly (1:4)–DMSO-d_6 mixtures.

In Fig. 8 the line width at the half-height of ^{13}C (chemical shifts are reported in Table S5) as a function of the DMSO-d_6 added for TBAB:Gly (1:4) is reported (for TBAB:Gly (1:3) see Fig. S6). Values for the peak width at the half-height of 90% TBAB:Gly (1:4)–10% DMSO-d_6 showed strong H-bonds between TBAB and Gly. However, with increasing DMSO-d_6 content in the sample, the supramolecular structure disintegrates similarly as with the addition of water to the DES sample (Fig. 5).

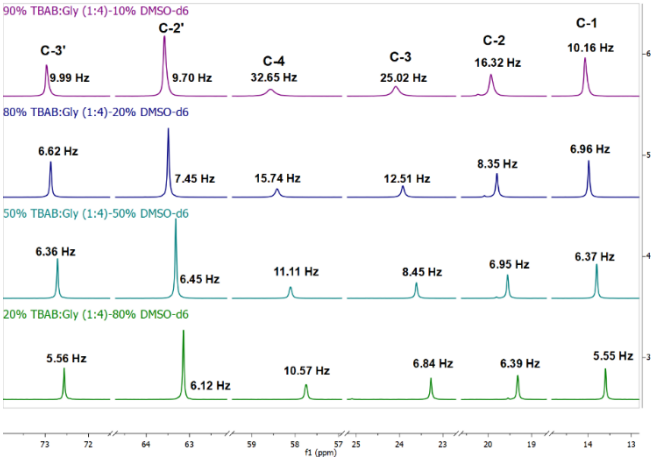

Fig. 8. ^{13}C NMR (150 MHz) spectra of TBAB:Gly (1:4)–DMSO-d_6 mixtures. For each peak the fwhm is reported. Spectra were recorded with 64 scans and processed using an exponential filter (LB = 5 Hz).

The previous findings are also confirmed by the evidence obtained using NOESY experiments (Fig. 9). The NOESY spectra of 80% TBAB:Gly (1:4)–20% DMSO-d_6 (Fig. 9a) and 80% TBAB:Gly (1:3)–20% DMSO-d_6 (Fig. S7a) mixtures shows positive NOESY cross-peaks originating from the interaction of TBAB and Gly, implying that H-bonds are still formed. With this composition, the supramolecular structure is preserved, as evidenced by the ROESY spectra, too (Fig. 9b and Fig. S7b). However, the

disintegration of the supramolecular structure is evident for the mixtures 50% TBAB:Gly (1:4)–50% DMSO-d_6 (Fig. 9c) and 50% TBAB:Gly (1:3)–50% DMSO-d_6 (Fig. S7c). NOESY spectra show negative cross-peaks between the protons of Gly and positive cross-peaks between the protons of TBAB (Fig. 9c and Fig. S7c). ROESY spectra show only intramolecular correlations (Fig. 9d and Fig. S7d).

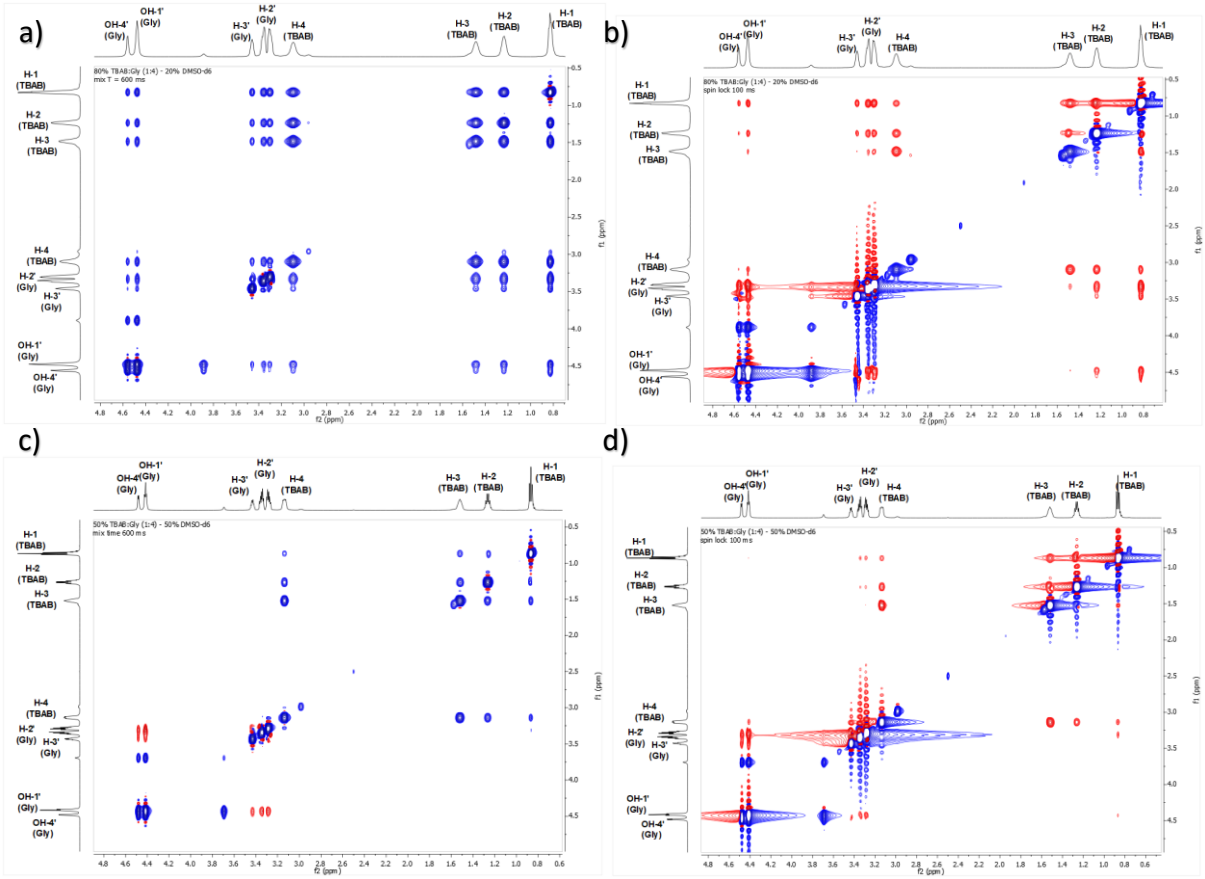

Fig. 9. NOESY (mix time 600 ms) (a, c) and ROESY (spin lock 100 ms) (b, d) spectra of 80% TBAB:Gly (1:4)–20% DMSO-d_6 (a, b) and 50% TBAB:Gly (1:4)–50% DMSO-d_6 (c, d).

3.2 Experimental and theoretical FT-IR analysis

In order to identify the functional groups that exist in DESs composed of TBAB and Gly in various molar ratios as well as the interaction between the HBA and HBD, FT-IR spectroscopy was used. The FT-IR spectra of TBAB:Gly (1:2), TBAB:Gly (1:3) and TBAB:Gly (1:4) compared with the spectra of pure TBAB and Gly are presented in Fig. 10.

In the TBAB spectrum (Fig. 10a), the C–H stretching vibrations of the $–CH_2$ and $–CH_3$ groups are observed around 2955–2872 cm^{-1}. Asymmetrical N–H stretching and C–N stretching are observed at 3415.2 cm^{-1} and 1021 cm^{-1}, respectively. The IR spectrum of the pure Gly (Fig. 10b) shows O–H stretching vibration at 3281.4 cm^{-1}, while C–H stretching vibrations are revealed by peaks in the region of 2878.6–2931.9 cm^{-1}. CH_2 bending is also observed in the region of 1500–1200 cm^{-1}. The bending of the C–O–H group is observed in the range from 1400 to 1420 cm^{-1}, and C–O stretching of the primary alcohol is observed at 1112 cm^{-1}.

The three DESs have very similar FT-IR spectra (Fig. 10 c-e) because the HBA and HBD are the same in each case in variable molar ratios. Therefore, no significant variations were observed between the DESs' spectra, except the stretching vibration band of the hydroxyl group. In all DESs' spectra, the O–H stretching overlapped with the N–H stretching. It can be seen that as the amount of Gly in the

DESs increases, the –OH bond shifts towards a lower wavenumber (from 3329.2 to 3322.8 cm^{-1}). This result can be explained by the formation of new hydrogen bonds in the vicinity of the –OH group (i.e. O–H···Br, O–H···O–H). The rest of the peaks from the DESs' spectra corresponding to the C–O–C (1180 cm^{-1}), C–O (1112 cm^{-1}), C–H of CH_2 (2960–2932 cm^{-1}) and CH_3 (2875.1 cm^{-1}) stretch stays in the same position. This indicates that these groups are not actively involved in the formation of hydrogen bonds. Similar behavior was also observed in other studies [29]. The wavenumber values of the characteristic peak shifts in FT-IR spectra are presented in Table S6.

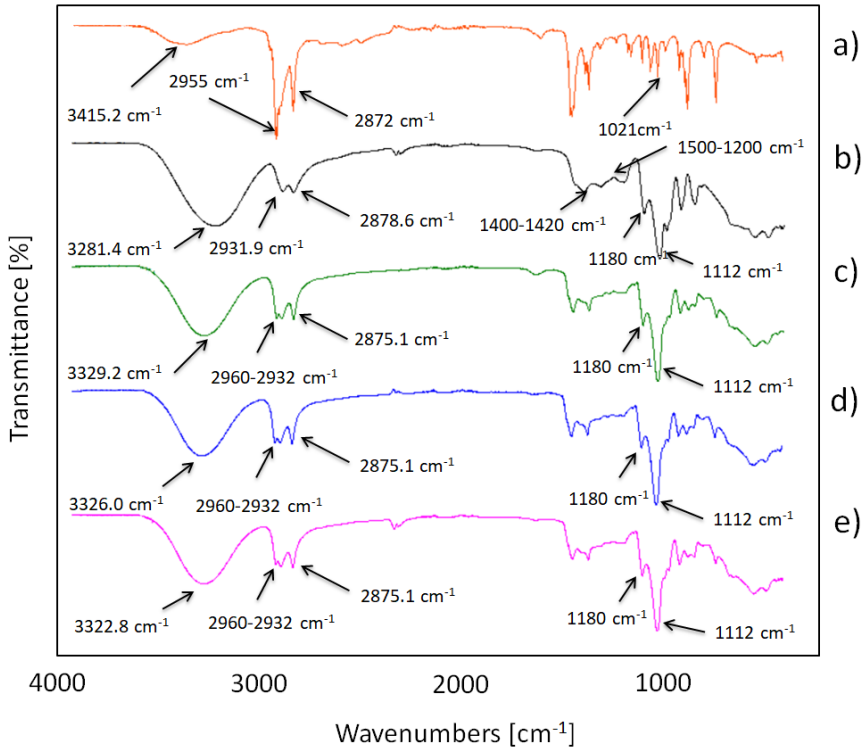

Fig. 10. FT-IR spectra of a) TBAB; b) Gly; c) TBAB:Gly (1:2); d) TBAB:Gly (1:3); e) TBAB:Gly (1:4).

The FT-IR spectrum for pure water contains two dominant peaks – at 1631.4 cm^{-1} and 3340.6 cm^{-1} (Fig. 11). The first peak, which is characterized by a sharp shape with moderate intensity can be assigned to scissoring bending. The second peak is characterized by a broader band and can be assigned to two overlapping asymmetrical and symmetrical stretching of the water molecule. When water was added to the TBAB:Gly (1:3 molar ratio), the O–H bands shifted to higher frequencies, towards the O–H stretching of the water molecule. With an increase in the amount of water in the DES, the frequencies of the O–H bands shift towards higher values, from 3326.2 cm^{-1} to 3353 cm^{-1}, 3388 cm^{-1} and 3340.6 cm^{-1}, respectively, for 50, 80 and 90% water addition. This result can be explained by the weakening of strong hydrogen bonds between the HBD and HBA. Similar behavior was observed earlier for other DESs [30, 31].

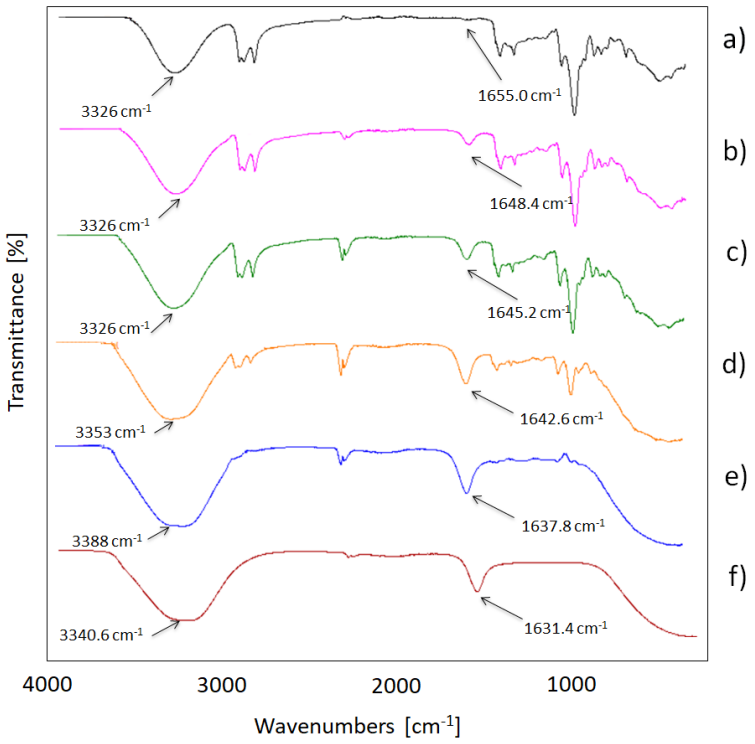

Fig. 11. FT-IR spectra of a) TBAB:Gly (1:3); b) 80% TBAB:Gly (1:3)–20% H_2O; c) 50% TBAB:Gly (1:3)–50% H_2O; d) 20% TBAB:Gly (1:3)–80% H_2O; e) 10% TBAB:Gly (1:3)–90% H_2O; f) pure H_2O.

In order to obtain the theoretical FT-IR spectra of the DESs, frequency calculation analyses were used. All calculations were performed for free DES molecules in a vacuum, while experimental studies were made for liquid samples. This causes differences between the calculated and observed vibrational wavenumbers [32]. The theoretical vibrational frequencies obtained by quantum chemical calculations are usually larger than the experimental values. The calculated results should be scaled by empirical scaling factors, which mainly depends on the method and basis sets used in the calculations [33]. In this study, empirical scaling factors of 0.958 and 0.983 were adopted for the wavenumbers in the range from 4000 to 1700 cm^{-1} and from 1700 to 500 cm^{-1}, respectively, based on previous studies [23]. The calculated wavenumbers after scaling are presented in Table S6. The largest difference between the theoretical and experimental results was 2.4 cm^{-1}. This accuracy indicates that the experimental, theoretical and literature results are highly consistent.

3.3 Raman spectroscopy

In the next step, experimental and theoretical Raman spectroscopy was used for better interpretation of the DES formation. Raman spectroscopy is rarely used to interpret DES structures. However, it is considered a better method compared to FT-IR, because the recorded peaks in the spectrum are narrower and the signals do not overlap [34]. Fig. 12 shows the Raman spectra of pure TBAB, Gly and the DESs. The broad band, at which the OH stretching of pure Gly appears, reveals two main bands centered at 3416 cm^{-1} and 3240 cm^{-1}. The same bands with lower intensity can be identified on the DES spectra at 3400 and 3231.2 cm^{-1}. The observed shifts to lower wavenumbers indicates a strengthening of the hydrogen bond in the DES structures [35]. However, increasing the Gly content does not change the position of the peak, which confirms the lack of additional hydrogen bonds in the DES structures. Broad bands with high intensity at 2996-2874 cm^{-1}, which can be assigned to C–H stretching vibrations of methyl and methylene group, are observed in all Raman spectra. The peaks observed in the range of 1499–1411 cm^{-1} can be assigned to the CH_2 scissors and CH_3 deformation

vibrations. The peaks at 1122 and 1069 can be assign to the CO stretch from C–3' and C–2', respectively. The peak at 906 and 874 cm^{-1} can be assigned to the NC_4 symmetric and asymmetric stench.

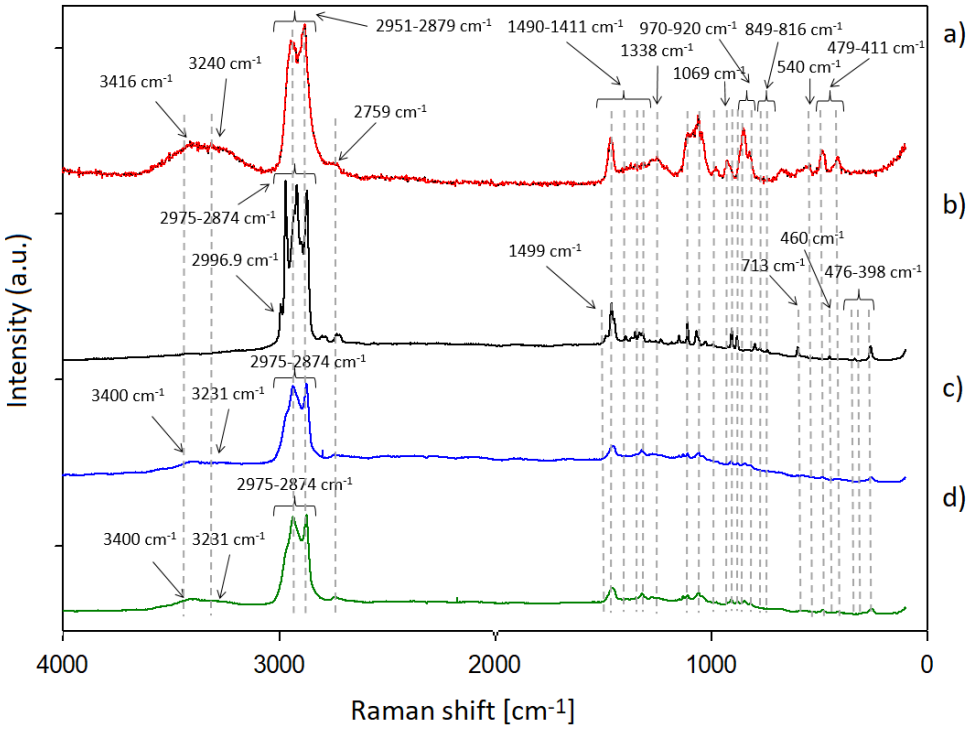

Fig. 12. Raman spectra of a) Gly; b) TBAB; c) TBAB:Gly (1:3); d) TBAB:Gly (1:4).

After the addition of water (Fig. 13) to the TBAB:Gly (1:3), a broad peak can be seen in the Raman spectrum from 3700 to 3040 cm^{-1}. This peak can be assigned to the asymmetric and symmetric OH stretch. As the water content increases, the peak intensity increases, while the intensity of the band components of Gly and TBAB decrease. The rest of peaks from the DESs' spectra stay in the same position after the addition of water. The detailed Raman peak identification and shift values are presented in Table S7.

Based on the peak shift in Raman spectroscopy, consistent results for the FT-IR studies were obtained. It has been proven that hydrogen bonds are formed between the TBAB and Gly molecules, leading to the DES formation. However, increasing the amount of Gly in the DES structure does not increase the number of hydrogen bonds in the DES structure. In the area of asymmetric and symmetric OH stretch in the DES-water complex, the intensity of the peaks increases as the amount of water increases. This indicates the formation of additional hydrogen bonds, which may form between Gly-Gly, Gly-water or water-water.

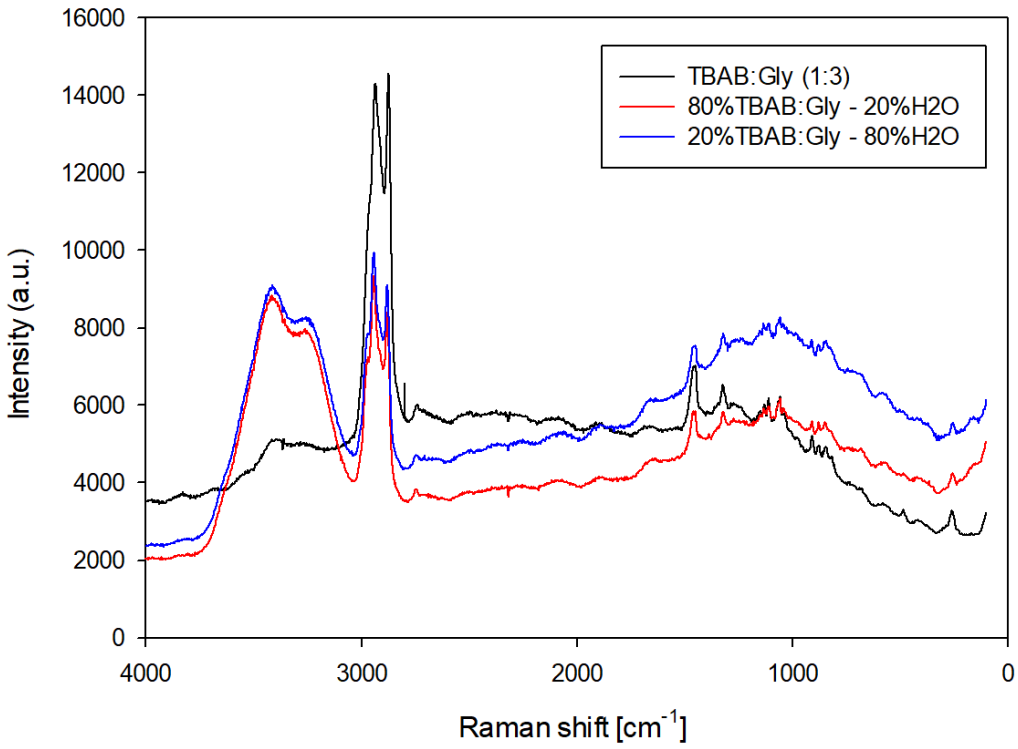

Fig. 13. Raman spectra of TBAB:Gly (1:3); 80% TBAB:Gly (1:3)–20% H_2O; 20% TBAB:Gly (1:3)–80% H_2O.

Conclusion

In the present paper, three deep eutectic solvents composed of TBAB and Gly in 1:2, 1:3 and 1:4 molar ratios were synthesized. Characterization of the DES structures and studies on the mechanism of their formation were carried on using NMR, FT-IR and Raman spectroscopy. In addition, the influence of the varying amounts of added water on the DES structures was also examined.

The obtained results indicate that the hydrogen bonds between TBAB and Gly exist in the DESs at all molar ratios. However, it was difficult to detect how many and where the hydrogen bonds occur. A small amount of water added to the DES structure provides the establishment of an H-bond network, which does not weaken the existing H-bonds between the HBA and HBD, thus creating a stable supramolecular structure. The H-bonds between TBAB and Gly are weakened by dilution with water. However, the supramolecular structure remains preserved to some extent even at 50% water content.

CRediT authorship contribution statement

Renáta Chromá: Investigation, Writing - Original Draft **Mária Vilková**: Methodology, Investigation, Data Curation, Writing - Original Draft, Writing - Review & Editing **Ivan Shepa**: Investigation **Patrycja Makoś-Chełstowska**: Formal analysis, Data Curation, Writing - Original Draft, Writing - Review & Editing **Vasil Andruch**: Conceptualization, Writing - Original Draft, Writing - Review & Editing, Supervision.

Acknowledgement

This work was supported by the Scientific Grant Agency of the Ministry of Education, Science, Research and Sport of the Slovak Republic (VEGA 1/0220/21). R.CH. would like to express her great gratitude to Dr. M. Vavra for his invaluable help in measuring the IR spectra.

References

[1] P.T. Anastas, M.M. Kirchhoff, Origins, current status, and future challenges of green chemistry, Acc. Chem. Res., 35 (2002) 686-694.
[2] P. Walden, Über die Molekulargrösse und elektrische Leitfähigkeit einiger geschmolzener Salze, Bull Acad Imper Sci (St Petersburg), (1914) 405-422.
[3] P.G. Jessop, L. Phan, A. Carrier, S. Robinson, C.J. Dürr, J.R. Harjani, A solvent having switchable hydrophilicity, Green Chem., 12 (2010) 809-814. 10.1039/b926885e
[4] G. Lasarte-Aragonés, R. Lucena, S. Cárdenas, M. Valcárcel, Use of switchable solvents in the microextraction context, Talanta, 131 (2014) 645-649. 10.1016/j.talanta.2014.08.031
[5] A.P. Abbott, D. Boothby, G. Capper, D.L. Davies, R.K. Rasheed, Deep Eutectic Solvents formed between choline chloride and carboxylic acids: Versatile alternatives to ionic liquids, J. Am. Chem. Soc., 126 (2004) 9142-9147. 10.1021/ja048266j
[6] A. Shishov, A. Bulatov, M. Locatelli, S. Carradori, V. Andruch, Application of deep eutectic solvents in analytical chemistry. A review, Microchem. J., 135 (2017) 33-38. 10.1016/j.microc.2017.07.015
[7] Z. Triaux, H. Petitjean, E. Marchioni, M. Boltoeva, C. Marcic, Deep eutectic solvent–based headspace single-drop microextraction for the quantification of terpenes in spices, Anal. Bioanal. Chem., 412 (2020) 933-948. 10.1007/s00216-019-02317-9
[8] W. Tang, Y. Dai, K.H. Row, Evaluation of fatty acid/alcohol-based hydrophobic deep eutectic solvents as media for extracting antibiotics from environmental water, Anal. Bioanal. Chem., 410 (2018) 7325-7336. 10.1007/s00216-018-1346-6
[9] A. Shishov, R. Chromá, C. Vakh, J. Kuchár, A. Simon, V. Andruch, A. Bulatov, In situ decomposition of deep eutectic solvent as a novel approach in liquid-liquid microextraction, Anal. Chim. Acta, 1065 (2019) 49-55. 10.1016/j.aca.2019.03.038
[10] A.K. El-Deen, K. Shimizu, Deep eutectic solvent as a novel disperser in dispersive liquid-liquid microextraction based on solidification of floating organic droplet (DLLME-SFOD) for preconcentration of steroids in water samples: Assessment of the method deleterious impact on the environment using Analytical Eco-Scale and Green Analytical Procedure Index, Microchem. J., 149 (2019). 10.1016/j.microc.2019.103988
[11] A. Shishov, N. Volodina, D. Nechaeva, S. Gagarinova, A. Bulatov, Deep eutectic solvents as a new kind of dispersive solvent for dispersive liquid-liquid microextraction, RSC Adv., 8 (2018) 38146-38149. 10.1039/c8ra07300g
[12] A. Shishov, P. Terno, L. Moskvin, A. Bulatov, In-syringe dispersive liquid-liquid microextraction using deep eutectic solvent as disperser: Determination of chromium (VI) in beverages, Talanta, 206 (2020) 120209. 10.1016/j.talanta.2019.120209
[13] S.M. Yousefi, F. Shemirani, S.A. Ghorbanian, Hydrophobic Deep Eutectic Solvents in Developing Microextraction Methods Based on Solidification of Floating Drop: Application to the Trace HPLC/FLD Determination of PAHs, Chromatographia, 81 (2018) 1201-1211. 10.1007/s10337-018-3548-7
[14] G.S. Kanberoglu, E. Yilmaz, M. Soylak, Application of deep eutectic solvent in ultrasound-assisted emulsification microextraction of quercetin from some fruits and vegetables, J. Mol. Liq., 279 (2019) 571-577. 10.1016/j.molliq.2019.01.130
[15] M. Soylak, S. Deryol, F. Uzcan, A new green microextraction method for traces Brown HT (E155) by using deep eutectic solvents prior to its spectrophotometric determination, Int. J. Environ. Anal. Chem., (2019). 10.1080/03067319.2019.1685092
[16] M. Soylak, F. Uzcan, A novel ultrasonication-assisted deep eutectic solvent microextraction procedure for tartrazine at trace levels from environmental samples, J. Iranian Chem. Soc., 17 (2020) 461-467. 10.1007/s13738-019-01781-5

[17] Z. Erbas, M. Soylak, E. Yilmaz, M. Dogan, Deep eutectic solvent based liquid phase microextraction of nickel at trace level as its diethyldithiocarbamate chelate from environmental samples, Microchem. J., 145 (2019) 745-750. 10.1016/j.microc.2018.11.039
[18] M. Vilková, J. Płotka-Wasylka, V. Andruch, The role of water in deep eutectic solvent-base extraction, J. Mol. Liq., 304 (2020). 10.1016/j.molliq.2020.112747
[19] S. Adams, P. De Castro, P. Echenique, J. Estrada, M.D. Hanwell, P. Murray-Rust, P. Sherwood, J. Thomas, J. Townsend, The Quixote Project: Collaborative and Open Quantum Chemistry data management in the internet age, Journal of Cheminformatics, 3 (2011). 10.1186/1758-2946-3-38
[20] F. Neese, The ORCA program system, Wiley Interdisciplinary Reviews: Computational Molecular Science, 2 (2012) 73-78. 10.1002/wcms.81
[21] S. Grimme, J. Antony, S. Ehrlich, H. Krieg, A consistent and accurate ab initio parametrization of density functional dispersion correction (DFT-D) for the 94 elements H-Pu, J. Chem. Phys., 132 (2010). 10.1063/1.3382344
[22] T. Lu, F. Chen, Multiwfn: A multifunctional wavefunction analyzer, J. Comput. Chem., 33 (2012) 580-592. 10.1002/jcc.22885
[23] S. Zhu, H. Li, W. Zhu, W. Jiang, C. Wang, P. Wu, Q. Zhang, H. Li, Vibrational analysis and formation mechanism of typical deep eutectic solvents: An experimental and theoretical study, J. Mol. Graphics Modell., 68 (2016) 158-175. 10.1016/j.jmgm.2016.05.003
[24] X. Zhu, H. Zhang, H. Li, The structure of water in dilute aqueous solutions of ionic liquids: IR and NMR study, J. Mol. Liq., 197 (2014) 48-51. 10.1016/j.molliq.2014.04.032
[25] A.J. Simpson, G. Woods, O. Mehrzad, Spectral editing of organic mixtures into pure components using NMR spectroscopy and ultraviscous solvents, Anal. Chem., 80 (2008) 186-194. 10.1021/ac702119d
[26] I. Delso, C. Lafuente, J. Muñoz-Embid, M. Artal, NMR study of choline chloride-based deep eutectic solvents, J. Mol. Liq., 290 (2019). 10.1016/j.molliq.2019.111236
[27] O.S. Hammond, D.T. Bowron, K.J. Edler, The Effect of Water upon Deep Eutectic Solvent Nanostructure: An Unusual Transition from Ionic Mixture to Aqueous Solution, Angewandte Chemie - International Edition, 56 (2017) 9782-9785. 10.1002/anie.201702486
[28] G.C. Dugoni, M.E. Di Pietro, M. Ferro, F. Castiglione, S. Ruellan, T. Moufawad, L. Moura, M.F. Costa Gomes, S. Fourmentin, A. Mele, Effect of Water on Deep Eutectic Solvent/β-Cyclodextrin Systems, ACS Sustain. Chem. Eng., 7 (2019) 7277-7285. 10.1021/acssuschemeng.9b00315
[29] M.K. Alomar, M. Hayyan, M.A. Alsaadi, S. Akib, A. Hayyan, M.A. Hashim, Glycerol-based deep eutectic solvents: Physical properties, J. Mol. Liq., 215 (2016) 98-103. 10.1016/j.molliq.2015.11.032
[30] S. Elderderi, C. Leman-Loubière, L. Wils, S. Henry, D. Bertrand, H.J. Byrne, I. Chourpa, C. Enguehard-Gueiffier, E. Munnier, A.A. Elbashir, L. Boudesocque-Delaye, F. Bonnier, ATR-IR spectroscopy for rapid quantification of water content in deep eutectic solvents, J. Mol. Liq., 311 (2020). 10.1016/j.molliq.2020.113361
[31] F. Gabriele, M. Chiarini, R. Germani, M. Tiecco, N. Spreti, Effect of water addition on choline chloride/glycol deep eutectic solvents: Characterization of their structural and physicochemical properties, J. Mol. Liq., 291 (2019). 10.1016/j.molliq.2019.111301
[32] M. Karabacak, M. Kurt, A. Ataç, Experimental and theoretical FT-IR and FT-Raman spectroscopic analysis of N1-methyl-2-chloroaniline, J. Phys. Org. Chem., 22 (2009) 321-330. 10.1002/poc.1480
[33] V. Krishnakumar, V. Balachandran, T. Chithambarathanu, Density functional theory study of the FT-IR spectra of phthalimide and N-bromophthalimide, Spectrochim. Acta Part A, 62 (2005) 918-925. 10.1016/j.saa.2005.02.051
[34] W.R. Carper, P.G. Wahlbeck, T.R. Griffiths, DFT models of molecular species in carbonate molten salts, J. Phys. Chem. B, 116 (2012) 5559-5567. 10.1021/jp3016694
[35] E. Mendelovici, R.L. Frost, T. Kloprogge, Cryogenic Raman spectroscopy of glycerol, Journal of Raman Spectroscopy, 31 (2000) 1121-1126. 10.1002/1097-4555(200012)31:12<1121::AID-JRS654>3.0.CO;2-G